Published in final edited form as:
Matrix Biol. 2012 July ; 31(6): 320–327. doi:10.1016/j.matbio.2012.05.002.

A Biomechanical Role for Perlecan in the Pericellular Matrix of Articular Cartilage

Rebecca E. Wilusz, M.S.[1,2], **Louis E. DeFrate, Ph.D.**[1,2], and **Farshid Guilak, Ph.D.**[1,2]
[1]Department of Orthopaedic Surgery, Duke University Medical Center
[2]Department of Biomedical Engineering, Duke University

Abstract

Chondrocytes are surrounded by a narrow pericellular matrix (PCM) that is biochemically, structurally, and biomechanically distinct from the bulk extracellular matrix (ECM) of articular cartilage. While the PCM is often defined by the presence of type VI collagen, other macromolecules such as perlecan, a heparan sulfate (HS) proteoglycan, are also exclusively localized to the PCM in normal cartilage and likely contribute to PCM structural integrity and biomechanical properties. Though perlecan is essential for normal cartilage development, its exact role in the PCM is unknown. The objective of this study was to determine the biomechanical role of perlecan in the articular cartilage PCM *in situ* and its potential as a defining factor of the PCM. To this end, atomic force microscopy (AFM) stiffness mapping was combined with dual immunofluorescence labeling of cryosectioned porcine cartilage samples for type VI collagen and perlecan. While there was no difference in overall PCM mechanical properties between type VI collagen- and perlecan-based definitions of the PCM, within the PCM, interior regions containing both type VI collagen and perlecan exhibited lower elastic moduli than more peripheral regions rich in type VI collagen alone. Enzymatic removal of HS chains from perlecan with heparinase III increased PCM elastic moduli both overall and locally in interior regions rich in both perlecan and type VI collagen. Heparinase III digestion had no effect on ECM elastic moduli. Our findings provide new evidence for perlecan as a defining factor in both the biochemical and biomechanical properties of the PCM.

Keywords

heparan sulfate; type VI collagen; chondron; atomic force microscopy; proteoglycan; chondrocyte; scanning probe microscope

1. Introduction

Within the extensive extracellular matrix (ECM) of articular cartilage, chondrocytes are surrounded by a narrow pericellular matrix (PCM) that together with the enclosed cell is referred to as a “chondron” (Poole et al., 1987). The PCM is distinct from the surrounding ECM in its biochemical composition [reviewed in (Poole, 1997)], ultrastructure (Hunziker et

Corresponding author: Farshid Guilak, Ph.D., Duke University Medical Center, Box 3093, Durham, NC 27710, Phone (919) 684-2521, Fax (919) 681-8490, guilak@duke.edu.

al., 1997; Poole et al., 1987), and biomechanical properties (Alexopoulos et al., 2003; Alexopoulos et al., 2005b; Darling et al., 2010; Wilusz et al., in press). While the exact function of the PCM in cartilage has yet to be determined, it is thought to play an important role in regulating the biomechanical microenvironment of the chondrocyte, protecting the cell during compressive loading (Poole et al., 1987) and serving as a mechanical transducer during joint loading (Guilak et al., 2006). Previous theoretical models (Alexopoulos et al., 2005a; Guilak and Mow, 2000; Korhonen and Herzog, 2008; Michalek and Iatridis, 2007) and experimental studies (Choi et al., 2007; Hing et al., 2002; Knight et al., 2001; Villanueva et al., 2009) have demonstrated that stress and strain in the vicinity of the chondrocyte is significantly influenced by the relative mechanical properties of the cell, PCM, and ECM.

In normal cartilage, the PCM is often defined by the exclusive presence and localization of type VI collagen around the chondrocyte (Poole et al., 1992; Poole et al., 1988). As such, previous studies investigating the biomechanical properties of the cartilage PCM have focused on type VI collagen and its role in PCM function. Using immunofluorescence-guided atomic force microscopy (AFM), a recent study demonstrated that PCM biomechanical properties correlated with the presence of type VI collagen and that matrix regions lacking type VI collagen immediately adjacent to the PCM exhibited higher elastic moduli than PCM regions rich in type VI collagen (Wilusz et al., in press). Alexopoulos and colleagues (Alexopoulos et al., 2009) demonstrated that intact chondrons can be isolated from Col6a1 knockout mice that lack type VI collagen and exhibit reduced mechanical properties as compared to wild-type controls. While these studies illustrate the important role of type VI collagen in the properties of the PCM, they also suggest that other PCM components likely contribute to its structural integrity and biomechanical properties.

A number of matrix molecules are found exclusively in the cartilage PCM as compared to the ECM including perlecan, a large heparan sulfate (HS) proteoglycan (Kvist et al., 2008; Melrose et al., 2006; Melrose et al., 2005; SundarRaj et al., 1995). Though its exact role in cartilage is unknown, perlecan is essential for normal cartilage development, and dysfunction of the perlecan gene results in skeletal dysplasias that are potentially lethal (Arikawa-Hirasawa et al., 1999; Costell et al., 1999; French et al., 1999; Gustafsson et al., 2003). Perlecan modulates signaling of multiple growth factors through its HS chains including the fibroblast growth factors (FGFs) (Aviezer et al., 1994; Chuang et al., 2010; Melrose et al., 2006; Smith et al., 2007; Vincent et al., 2007; Whitelock et al., 2008; Whitelock et al., 1996), and has been implicated in cell-matrix interactions (Kirn-Safran et al., 2009; SundarRaj et al., 1995) and matrix organization (Melrose et al., 2008). Importantly, perlecan demonstrates a strong electrostatic binding affinity for type VI collagen through its HS chains (Tillet et al., 1994) and interacts with fibronectin and laminin via its core protein and through charge interactions with its HS chains (Hopf et al., 1999; Hopf et al., 2001). Through these interactions, perlecan may have an important role in the structural organization and stabilization of the cartilage PCM.

The objective of this study was to determine the biomechanical role of perlecan in the PCM of articular cartilage and its potential role as a defining factor of the PCM. Cryosections of porcine articular cartilage samples were labeled for type VI collagen and perlecan using dual immunofluorescence (IF). Guided by IF labeling, AFM-based stiffness mapping (Darling et al., 2010; Wilusz et al., in press) was used to evaluate the elastic properties of matched PCM and ECM regions and correlate these properties with PCM biochemical composition. Enzymatic removal of HS chains from perlecan using heparinase III was performed to evaluate the functional role of HS in the biomechanical properties of cartilage. These methods were used to test the hypotheses that the presence of perlecan can be used to define the boundaries of the PCM, that PCM regions rich in perlecan exhibit lower elastic moduli

than regions lacking perlecan and that enzymatic removal of HS significantly reduces the microscale elastic properties of the PCM while having no effect on ECM properties.

2. Results

2.1 Immunofluorescence for type VI collagen and perlecan in porcine cartilage

IF labeling of cartilage sections revealed a consistent presence of both type VI collagen and perlecan immediately surrounding cell-sized voids. PCM labeling for type VI collagen was uniform throughout the tissue depth (Figure 1A). Type VI collagen was also found to be faintly dispersed in the ECM in the deep zone. Perlecan labeling was exclusively pericellular and more pronounced in the middle and deep zones of the cartilage as compared to the superficial zone (Figure 1B).

2.2 AFM stiffness mapping of type VI collagen and perlecan dual-labeled porcine cartilage PCM

Stiffness mapping revealed that type VI collagen, perlecan, and low elastic moduli localize in the pericellular region around cell-sized voids (Figure 2A, B, C, D). No difference in overall PCM elastic moduli was observed between type VI collagen-based (71 ± 3 kPa) and perlecan-based (68 ± 3 kPa) definitions of the PCM ($p = 0.70$; Figure 2E). Elastic moduli of the local ECM (93 ± 7 kPa) were significantly greater than PCM moduli using either biochemical definition ($p < 0.005$).

Type VI collagen and perlecan co-localized over 64 ± 3% of labeled PCM areas (positive for either type VI collagen or perlecan) and occupied inner regions of the PCM (Figure 3A, B). Regions positive for type VI collagen alone occupied 31 ± 4% of labeled PCM areas and were located in peripheral regions of the PCM. Within the PCM, elastic moduli in dual-labeled regions (68 ± 3 kPa) were significantly lower than moduli in regions positive for type VI collagen alone (81 ± 5 kPa; $p < 0.05$; Figure 2F). PCM regions positive for perlecan alone occupied 4 ± 1% of the labeled PCM area, with only 9 of the 23 sites tested having regions consisting of sufficient area on the stiffness map for analysis. Of these perlecan alone regions, 6 spanned the width of small portions of the evaluated PCM, occupying up to 18% of the total labeled PCM area, and 3 were located on the PCM periphery. Perlecan alone regions exhibited greater elastic moduli (92 ± 7 kPa) than dual-labeled regions ($p < 0.01$). There was no difference in elastic moduli between PCM regions positive for type VI collagen alone and perlecan alone ($p = 0.19$). Spatial mapping demonstrated that lower modulus regions were located within 1.0 μm of the PCM inner edge ($p < 0.05$) where 92 – 95% of the labeled area was dual-labeled for perlecan and type VI collagen (Figure 3C, D).

2.3 Immunofluorescence for 3G10, perlecan, and type VI collagen and histological staining analyses of heparinase III-digested porcine cartilage

Enzymatic digestion of HS with heparinase III was specific to PCM regions immediately surrounding cell-sized voids in cartilage sections. IF labeling for the heparinase III-specific HS epitope 3G10 matched the pericellular distribution of perlecan (Figure 4A, B, C) and co-localized with type VI collagen (Figure 4D, E, F). There was no 3G10 labeling present in undigested controls (data not shown). Digestion had no effect on IF labeling of either perlecan or type VI collagen (Figure 4G, H, I). Digestion with heparinase III did not induce a global loss of GAGs in cartilage sections (Figure 5A, B).

2.4 Effect of heparinase III digestion on the micromechanical properties of porcine cartilage PCM and ECM

Digestion with heparinase III resulted in a significant increase in the overall elastic modulus of the PCM as defined by perlecan labeling (69 ± 5 kPa vs. 56 ± 3 kPa; $p < 0.05$; Figure

6A). There was a trend toward an increase in PCM properties as defined by the presence of type VI collagen with digestion (70 ± 4 kPa vs. 60 ± 3 kPa; $p = 0.05$). There were no differences in the relative composition of tested control and digested PCM regions, with dual-labeled, type VI collagen alone and perlecan alone regions consisting of 60 ± 3%, 34 ± 3%, and 5 ± 1% of labeled areas in control PCM regions and 59 ± 3%, 37 ± 3%, and 3 ± 1% of labeled areas in digested PCM regions, respectively ($p > 0.39$). There was no significant change in ECM properties with heparinase III digestion as compared to undigested controls (103 ± 6 kPa vs. 93 ± 6 kPa; $p = 0.39$; Figure 5C).

Within the PCM, enzymatic removal of HS resulted in a significant increase in the elastic modulus of dual-labeled regions as compared to undigested controls (68 ± 5 kPa vs. 55 ± 2 kPa; $p < 0.05$; Figure 6B). There was no change in the properties of regions positive for type VI collagen alone (74 ± 4 kPa vs. 68 ± 4 kPa; $p = 0.31$). 15 of the 25 PCM regions tested in undigested controls and 13 of the 25 PCM regions tested in digested samples had perlecan alone regions consisting of sufficient area on the stiffness map for analysis. Of these perlecan alone regions, 16 spanned the width of small portions of the evaluated PCM, occupying up to 33% of the total labeled PCM area, and 13 were located on the PCM periphery. In these regions, there was a trend toward a significant increase in elastic moduli with digestion (87 ± 6 kPa vs. 74 ± 5 kPa; $p = 0.09$). In heparinase III digested PCM, dual-labeled regions exhibited elastic moduli similar to those of regions occupied by type VI collagen alone ($p = 0.94$) but lower than perlecan alone areas ($p < 0.01$). In undigested controls, dual-labeled regions were significantly softer than regions positive for either type VI collagen or perlecan alone ($p < 0.05$) and there was no difference observed between type VI collagen and perlecan alone regions ($p = 0.34$). Spatial mapping demonstrated significant increases in elastic moduli with digestion in regions within 1.0 μm of the PCM inner edge ($p < 0.05$; Figure 7A) where 80 – 85% of the labeled area was dual-labeled for perlecan and type VI collagen and 4 – 8% was positive for perlecan alone (Figure 7B).

3. Discussion

Our results provide new evidence for a biomechanical role for perlecan in the cartilage PCM. IF-guided AFM stiffness mapping revealed localization of perlecan, type VI collagen and low elastic moduli to the pericellular region around cell-sized voids. While there was no difference in overall PCM mechanical properties between type VI collagen- and perlecan-based definitions of the PCM, interior regions within the PCM containing both type VI collagen and perlecan exhibited lower elastic moduli than more peripheral regions rich in type VI collagen alone. Contrary to our initial hypothesis, enzymatic removal of HS chains from perlecan with heparinase III resulted in increased elastic moduli in the PCM, specifically in interior regions positive for both perlecan and type VI collagen. Heparinase III digestion had no effect on the micromechanical properties of the ECM.

AFM measures highly localized mechanical properties *in situ* that may be dominated by individual molecular components of the tissue. Therefore, our findings provide evidence for variations of elastic moduli within the PCM that are related to site-specific biochemical composition. PCM regions rich in perlecan and type VI collagen were located immediately adjacent to cell-sized voids and exhibited lower elastic moduli than more peripheral PCM regions rich in type VI collagen alone. Previous work by Loparic and colleagues investigating the nanostiffness of porcine articular cartilage with AFM (Loparic et al., 2010) demonstrated that proteoglycans *in situ* are an order of magnitude softer than collagen fibers. The low elastic moduli observed at the PCM interior in the present work were likely due to the high concentration of HS in this region, further supported by the increase elastic moduli in these regions with digestion of HS by heparinase III. In this regard, our results

suggest heparinase III digestion could be utilized to selectively manipulate the biochemical and biomechanical properties of the PCM with minimal effect on the surrounding ECM.

The exact mechanism by which perlecan contributes to lower elastic moduli is not understood. Proteoglycans are known to have lower compressive moduli than collagen fibers, due in part to their glycosaminoglycan side chains (Loparic et al., 2010). The HS chains of perlecan may contribute to lower elastic moduli in a manner analogous to a softer spring in series with a stiffer spring, where the effective spring constant of the system is lower than that spring constant of either component. In this respect, digestion of the HS chains exposes the stiffer underlying components of the solid matrix, thereby increasing the observed elastic moduli of these regions.

The localization of perlecan to low modulus, interior regions of the PCM provides support for a potential role for HS and perlecan in mechanotransduction in cartilage. Perlecan has been shown to regulate the bioactivity of FGFs through interaction with HS, serving as an extracellular store and mediating FGF binding to, and subsequent activation of, FGF receptor tyrosine kinases (Aviezer et al., 1994; Chuang et al., 2010; Melrose et al., 2006; Smith et al., 2007; Whitelock et al., 1996). Loading-induced activation of extracellularly regulated kinase (ERK) in cartilage (Vincent et al., 2002; Vincent et al., 2004) has been shown to depend on the presence and concentration of FGF-2 in the pericellular matrix (Vincent et al., 2007). Vincent and colleagues hypothesized that in unloaded cartilage, FGF-2 bound to HS chains of perlecan is sequestered away from the cell surface and that matrix deformation presents HS-bound FGF-2 to its receptor on the cell surface, activating downstream signaling pathways (Vincent et al., 2007). Since the cartilage PCM is significantly less stiff than the ECM, it experiences significant stress and strain amplification during mechanical loading and undergoes larger deformations than the surrounding ECM (Choi et al., 2007; Guilak and Mow, 2000). Localization of perlecan to low modulus regions in the PCM interior, as observed in the current study, would facilitate HS-bound FGF signaling via this proposed mechanism. Furthermore, perlecan may transmit mechanical signals directly to the chondrocyte via core protein interactions with cell surface integrins (Brown et al., 1997; Hayashi et al., 1992; Melrose et al., 2008).

The territorial matrix (TM) has been defined as a structural transition region between type VI collagen microfilaments in the PCM and type II collagen fibers in the ECM (Poole et al., 1984). Since there are no distinct structural boundaries among these three matrix regions, identification of the TM is difficult and often based on qualitative differences in proteoglycan content and collagen architecture (Hunziker et al., 1997; Poole et al., 1982; Poole et al., 1984, 1987; Poole et al., 1997). While type VI collagen is considered the defining boundary of the PCM in articular cartilage (Poole et al., 1988), type VI collagen has been reported to be present in the TM where it is interwoven with type II collagen fibrils (Soder et al., 2002). Given the exclusive localization of perlecan to the PCM observed here and in previous studies (Kvist et al., 2008; Melrose et al., 2006; Melrose et al., 2005; SundarRaj et al., 1995) and the distinct mechanical properties of regions positive for perlecan and type VI collagen in the immediate vicinity of the chondrocyte, our results suggest a defining role for perlecan as the boundary of the PCM with regions of type VI collagen alone representing the transition to the adjacent TM.

The fact that intact chondrons can be isolated from Col6a1 null mice (Alexopoulos et al., 2009) suggests that molecular components other than type VI collagen may provide alternative composition-based definitions of the PCM. In the present study, we focused on perlecan due to its exclusive presence to the PCM and documented roles in cartilage development and growth factor signaling. A number of other matrix molecules are found exclusively or at higher concentrations in the PCM as compared to the surrounding ECM,

including hyaluronan (Cohen et al., 2003; Knudson, 1993), biglycan (Kavanagh and Ashhurst, 1999), type IX collagen (Poole et al., 1997), fibronectin (Chang et al., 1997; Martin et al., 2002), and laminin (Durr et al., 1996; Kvist et al., 2008), and are known to interact with type VI collagen (Kielty et al., 1992; Wiberg et al., 2002) and perlecan (Hopf et al., 1999; Hopf et al., 2001; Kirn-Safran et al., 2009). These molecules likely contribute to PCM structure and biomechanical function.

The aim of this study was to characterize the biomechanical properties of articular cartilage PCM at the microscale. When using micrometer-sized spherical indenters as presented here, there are limitations in the lateral resolution of AFM-based indentation of soft substrates (Dimitriadis et al., 2002; Radmacher et al., 1992). From Hertz contact mechanics, the contact radius of a spherical probe scales with tip radius and indentation depth. Since a force threshold (300 nN) was used for all stiffness mapping, indentation depths were not equivalent throughout a single scan region. Indentations were larger in the soft interior of the PCM and smaller in stiff peripheral PCM, TM, and ECM regions. As a result, contact radii were larger in PCM regions (~2.0 μm) as compared to ECM regions (~1.5 μm). This contact footprint would have masked the sharp transition in matrix stiffness between the PCM and ECM proposed in theoretical models (Alexopoulos et al., 2005a; Guilak and Mow, 2000; Korhonen and Herzog, 2008; Michalek and Iatridis, 2007). In addition, contact with adjacent TM and/or ECM regions during indentation may have contributed to artificial stiffening of peripheral PCM regions. Nonetheless, the elastic moduli measured for the PCM in this study are highly consistent with previous studies using AFM (Darling et al., 2010; Wilusz et al., in press) as well as other techniques such as micropipette aspiration (Alexopoulos et al., 2003), and inverse computational methods (Kim et al., 2010).

In summary, this study provides support for perlecan as a defining factor in both the biochemical and biomechanical boundaries of the PCM. The HS chains of perlecan soften the PCM in the immediate vicinity of the chondrocyte and presumably, generate an environment conducive for mechanotransduction via HS-bound growth factors or direct cell-matrix interactions. By demonstrating site-specific differences in mechanical properties coincident with spatial variations in biochemical composition, our findings provide a more complete characterization of the chondrocyte microenvironment in articular cartilage.

4. Methods

4.1 Tissue sample preparation

Full thickness articular cartilage samples were collected from central regions of the medial femoral condyle of skeletally mature, macroscopically normal female pig knee joints. Cartilage samples were wrapped in phosphate-buffered saline (PBS)-soaked gauze and frozen at −20°C for intermediate storage. Samples were embedded in water-soluble embedding medium (Tissue-Tek O.C.T. Compound; Sakura Finetek USA, Inc., Torrance, CA) and sectioned perpendicular to the articular surface in 5 μm-thick slices using a cryostat microtome (Leica CM1850; Leica Microsystems, Inc., Buffalo Grove, IL). Cartilage slices were collected on negatively charged glass slides and washed thoroughly with PBS to remove the water-soluble embedding medium prior to IF labeling and AFM testing.

4.2 Immunofluorescence for type VI collagen and perlecan

Unfixed cartilage sections were simultaneously labeled for type VI collagen and perlecan. Sections were blocked in 10% normal goat serum (Invitrogen, Carlsbad, CA) for 20 minutes at room temperature. Samples were incubated with primary antibodies for type VI collagen (anti-collagen type VI raised in rabbit, 70R-CR009X, Fitzgerald Industries International, Inc., Action, MA) and perlecan (anti-perlecan raised in rat, sc-33707, Santa Cruz Biotechnology, Inc., Santa Cruz, CA) at a 1:50 dilution in 10% goat serum for 20 minutes at

room temperature. After three PBS washes of 5 minutes each, samples were incubated with secondary antibodies (AlexaFluor 568 goat anti-rabbit IgG and AlexaFluor 488 goat anti-rat IgG, Invitrogen) at a 1:200 dilution in 10% goat serum for 20 minutes in the dark at room temperature. Sections were rinsed twice in PBS for 5 minutes each and remained in PBS at room temperature during AFM testing.

4.3 Enzymatic digestion of heparan sulfate with heparinase III

Heparinase III (heparitinase I; EC 4.2.2.8; Sigma-Aldrich, Inc., St. Louis, MO) is the most specific heparinase for HS, demonstrating no activity for heparin (Ernst et al., 1995). Cartilage sections were incubated in 50 μL of 6 U/mL (0.01 IU/mL) heparinase III solution in 20 mM Tris-HCl containing 0.1 mg/mL bovine serum albumin (BSA) and 4 mM $CaCl_2$, pH 7.0 at 37°C for 30 minutes. Undigested control sections were incubated at 37°C for 30 minutes in enzyme buffer.

Digestion was confirmed using IF for the heparinase III-specific HS epitope 3G10 (mouse monoclonal primary antibody H1890-75, US Biological, Swampscott, MA) (David et al., 1992) on undigested control and digested sections. Dual IF labeling was used to evaluate localization of the HS epitope to the cartilage PCM using the protocol outlined in Section 4.2 (secondary antibody AlexaFluor 488/568 goat anti-mouse IgG, Invitrogen). Cartilage sections were simultaneously labeled with antibodies for 3G10 and type VI collagen to determine if digested HS was found exclusively in the PCM. To confirm that digested HS was associated with perlecan, sections were dual-labeled with antibodies for 3G10 and perlecan. It is important to note that the monoclonal antibody used to label perlecan was raised against the core protein of perlecan and thus was not expected to be affected by heparinase III digestion. Control experiments were performed to confirm this result and no difference was observed between the IF labeling of undigested perlecan and heparinase III-digested perlecan on adjacent sections from the same porcine cartilage specimens (data not shown). Histological staining with Safranin-O (proteoglycans) and fast green (collagen) was used to visualize global loss of proteoglycans from sections with digestion.

For AFM testing, sample-matched undigested control and heparinase III-digested sections were dual-labeled for type VI collagen and perlecan as described in section 4.2. Sections remained in PBS at room temperature during testing.

4.4 Mechanical characterization via AFM stiffness mapping

Simultaneous force measurements and fluorescence imaging were performed using an AFM system (MFP-3DBio; Asylum Research, Santa Barbara, CA) integrated with an inverted fluorescence microscope (AxioObserver A1; Carl Zeiss, Inc., Thornwood, NY). For microscale indentation, borosilicate glass spheres (5 μm diameter) were attached to tipless AFM cantilevers ($k \approx 4.5$ N/m; Novascan Technologies, Inc., Ames, IA). Indentations were applied with a force trigger of 300 nN and curves were sampled at 7.5 kHz. For evaluation of PCM elastic properties, indentations (1600 sites/region, 15 μm/s indentation velocity) were sequentially applied over a 20 μm × 20 μm region of interest defined by microscopic examination with phase contrast imaging and positive IF labeling around cell-sized voids. Images of perlecan (green) and type VI collagen (red) labeling were captured for each PCM region. Topographical maps of relative height were also collected during elastic mapping of each PCM scan region. Elastic properties of the adjacent ECM were evaluated using the same approach over 20 μm × 20 μm regions visually devoid of PCM (16 indentations/region, 15 μm/s indentation velocity). For all samples, AFM testing was completed within 4 hours of initial sectioning.

To evaluate the spatial relationship between biochemical composition and biomechanical properties within the PCM *in situ,* paired PCM/ECM regions (n = 23 total regions) were selected in the middle/deep zone (200 – 400 μm from the articular surface) of each cartilage sample (N = 4 pigs). To evaluate the biomechanical role of HS in the cartilage PCM, site-matched PCM/ECM regions were evaluated in the middle/deep zone of paired undigested and heparinase III-digested cartilage sections (N = 6 pigs, n = 25 total regions).

4.5 Data analysis

Raw data for cantilever deflection and z-piezo movement were collected and analyzed using a custom MATLAB script (The MathWorks, Natick, MA). Elastic moduli, *E*, were determined by fitting a modified Hertz model to force-indentation curves as described previously (Darling et al., 2006). For articular cartilage, the local Poisson's ratio, ν, was assumed to be 0.04 for both the ECM (Chen et al., 2001; Choi et al., 2007; Mow et al., 1980) and PCM (Alexopoulos et al., 2005b). Probe-surface contact was identified using contact point extrapolation, as described previously (Guo and Akhremitchev, 2006). Hertzian contact mechanics provided excellent fits to the experimental data for all force-indentation curves ($R^2 > 0.90$). Two-dimensional contour maps were generated of the spatial distribution of calculated elastic moduli in each region.

The cartilage PCM was defined based on positive IF labeling around cell-sized voids and data were included for all indentations that fell within labeled regions. ImageJ (National Institutes of Health) was used to crop collected images to produce single channel IF images of each PCM scan region (Figure 2A, B; overlaid in Figure 2C). For each PCM scan region, two IF images (green, red) and the corresponding topographical and elastic moduli contour maps were imported into Mathematica for alignment, as described previously (Wilusz et al., in press). Once aligned, IF images were converted to binary masks to indicate regions of positive staining for each individual channel using an optimal threshold value determined from range of IF images. IF-positive masks and elastic moduli contour maps were analyzed in MATLAB to extract PCM data for each scan region. Using single channel masks, overall PCM moduli were evaluated based on the presence of type VI collagen or perlecan. Relative staining areas for dual-labeled, type VI collagen alone, and perlecan alone regions within the PCM were determined by overlaying the single channel masks. Elastic properties were evaluated for each of these IF-defined regions. To quantitatively evaluate the spatial distribution of moduli in the chondrocyte microenvironment, the stiffness progression of PCM moduli was evaluated in radial increments of 0.5 μm from the PCM inner edge. The same analysis was performed on overlaid IF masks to determine the relative composition of the PCM within each radial increment.

4.6 Statistical analyses

Differences between ECM and PCM elastic moduli were evaluated using a one-way ANOVA (matrix region) and Fisher's LSD *post-hoc* test ($\alpha = 0.05$). Differences among IF-defined regions within the PCM (dual-labeled, type VI collagen alone, perlecan alone) were evaluated using a one-way ANOVA (IF labeling) and Fisher's LSD *post-hoc* test ($\alpha = 0.05$). Stiffness progression data were evaluated using a one-way ANOVA (distance) and Fisher's LSD *post-hoc* test ($\alpha = 0.05$).

The effect of HS-digestion with heparinase III on ECM elastic moduli was evaluated using a Student's *t*-test ($\alpha = 0.05$). Significant differences in overall PCM elastic moduli with digestion between type VI collagen- and perlecan-based definitions were evaluated using two-way ANOVA (PCM definition, digestion) and Fisher's LSD *post-hoc* test ($\alpha = 0.05$). Significant differences in stained PCM areas and elastic moduli among IF labeled regions within the PCM with heparinase III digestion were evaluated using two-way ANOVA (IF

labeling, digestion) and Fisher's LSD *post-hoc* test ($\alpha = 0.05$). Differences between control and digested elastic moduli were evaluated separately for each 0.5 μm increment in the outward stiffness progression using a Student's *t*-test ($\alpha = 0.05$). All data are presented as mean ± standard error.

Acknowledgments

The authors would like to thank Dr. Holly Leddy for helpful discussions. This work was supported in part by a National Science Foundation Graduate Research Fellowship (REW) and National Institutes of Health grants AG15768, AR50245, AR48182, AR48852, and AR055659.

References

Alexopoulos LG, Haider MA, Vail TP, Guilak F. Alterations in the mechanical properties of the human chondrocyte pericellular matrix with osteoarthritis. J Biomech Eng. 2003; 125:323–333. [PubMed: 12929236]

Alexopoulos LG, Setton LA, Guilak F. The biomechanical role of the chondrocyte pericellular matrix in articular cartilage. Acta biomaterialia. 2005a; 1:317–325. [PubMed: 16701810]

Alexopoulos LG, Williams GM, Upton ML, Setton LA, Guilak F. Osteoarthritic changes in the biphasic mechanical properties of the chondrocyte pericellular matrix in articular cartilage. Journal of biomechanics. 2005b; 38:509–517. [PubMed: 15652549]

Alexopoulos LG, Youn I, Bonaldo P, Guilak F. Developmental and osteoarthritic changes in Col6a1-knockout mice: biomechanics of type VI collagen in the cartilage pericellular matrix. Arthritis Rheum. 2009; 60:771–779. [PubMed: 19248115]

Arikawa-Hirasawa E, Watanabe H, Takami H, Hassell JR, Yamada Y. Perlecan is essential for cartilage and cephalic development. Nature genetics. 1999; 23:354–358. [PubMed: 10545953]

Aviezer D, Hecht D, Safran M, Eisinger M, David G, Yayon A. Perlecan, basal lamina proteoglycan, promotes basic fibroblast growth factor-receptor binding, mitogenesis, and angiogenesis. Cell. 1994; 79:1005–1013. [PubMed: 7528102]

Brown JC, Sasaki T, Gohring W, Yamada Y, Timpl R. The C-terminal domain V of perlecan promotes beta1 integrin-mediated cell adhesion, binds heparin, nidogen and fibulin-2 and can be modified by glycosaminoglycans. Eur J Biochem. 1997; 250:39–46. [PubMed: 9431988]

Chang J, Nakajima H, Poole CA. Structural colocalisation of type VI collagen and fibronectin in agarose cultured chondrocytes and isolated chondrons extracted from adult canine tibial cartilage. Journal of anatomy. 1997; 190 (Pt 4):523–532. [PubMed: 9183676]

Chen SS, Falcovitz YH, Schneiderman R, Maroudas A, Sah RL. Depth-dependent compressive properties of normal aged human femoral head articular cartilage: relationship to fixed charge density. Osteoarthritis and cartilage / OARS, Osteoarthritis Research Society. 2001; 9:561–569.

Choi JB, Youn I, Cao L, Leddy HA, Gilchrist CL, Setton LA, Guilak F. Zonal changes in the three-dimensional morphology of the chondron under compression: the relationship among cellular, pericellular, and extracellular deformation in articular cartilage. Journal of biomechanics. 2007; 40:2596–2603. [PubMed: 17397851]

Chuang CY, Lord MS, Melrose J, Rees MD, Knox SM, Freeman C, Iozzo RV, Whitelock JM. Heparan sulfate-dependent signaling of fibroblast growth factor 18 by chondrocyte-derived perlecan. Biochemistry. 2010; 49:5524–5532. [PubMed: 20507176]

Cohen M, Klein E, Geiger B, Addadi L. Organization and adhesive properties of the hyaluronan pericellular coat of chondrocytes and epithelial cells. Biophysical journal. 2003; 85:1996–2005. [PubMed: 12944312]

Costell M, Gustafsson E, Aszodi A, Morgelin M, Bloch W, Hunziker E, Addicks K, Timpl R, Fassler R. Perlecan maintains the integrity of cartilage and some basement membranes. J Cell Biol. 1999; 147:1109–1122. [PubMed: 10579729]

Darling EM, Wilusz RE, Bolognesi MP, Zauscher S, Guilak F. Spatial mapping of the biomechanical properties of the pericellular matrix of articular cartilage measured in situ via atomic force microscopy. Biophysical journal. 2010; 98:2848–2856. [PubMed: 20550897]

Darling EM, Zauscher S, Guilak F. Viscoelastic properties of zonal articular chondrocytes measured by atomic force microscopy. Osteoarthritis and cartilage / OARS, Osteoarthritis Research Society. 2006; 14:571–579.

David G, Bai XM, Van der Schueren B, Cassiman JJ, Van den Berghe H. Developmental changes in heparan sulfate expression: in situ detection with mAbs. J Cell Biol. 1992; 119:961–975. [PubMed: 1385449]

Dimitriadis EK, Horkay F, Maresca J, Kachar B, Chadwick RS. Determination of elastic moduli of thin layers of soft material using the atomic force microscope. Biophysical journal. 2002; 82:2798–2810. [PubMed: 11964265]

Durr J, Lammi P, Goodman SL, Aigner T, von der Mark K. Identification and immunolocalization of laminin in cartilage. Exp Cell Res. 1996; 222:225–233. [PubMed: 8549667]

Ernst S, Langer R, Cooney CL, Sasisekharan R. Enzymatic degradation of glycosaminoglycans. Crit Rev Biochem Mol Biol. 1995; 30:387–444. [PubMed: 8575190]

French MM, Smith SE, Akanbi K, Sanford T, Hecht J, Farach-Carson MC, Carson DD. Expression of the heparan sulfate proteoglycan, perlecan, during mouse embryogenesis and perlecan chondrogenic activity in vitro. J Cell Biol. 1999; 145:1103–1115. [PubMed: 10352025]

Guilak F, Alexopoulos LG, Upton ML, Youn I, Choi JB, Cao L, Setton LA, Haider MA. The pericellular matrix as a transducer of biomechanical and biochemical signals in articular cartilage. Annals of the New York Academy of Sciences. 2006; 1068:498–512. [PubMed: 16831947]

Guilak F, Mow VC. The mechanical environment of the chondrocyte: a biphasic finite element model of cell-matrix interactions in articular cartilage. Journal of biomechanics. 2000; 33:1663–1673. [PubMed: 11006391]

Guo S, Akhremitchev BB. Packing density and structural heterogeneity of insulin amyloid fibrils measured by AFM nanoindentation. Biomacromolecules. 2006; 7:1630–1636. [PubMed: 16677048]

Gustafsson E, Aszodi A, Ortega N, Hunziker EB, Denker HW, Werb Z, Fassler R. Role of collagen type II and perlecan in skeletal development. Annals of the New York Academy of Sciences. 2003; 995:140–150. [PubMed: 12814946]

Hayashi K, Madri JA, Yurchenco PD. Endothelial cells interact with the core protein of basement membrane perlecan through beta 1 and beta 3 integrins: an adhesion modulated by glycosaminoglycan. J Cell Biol. 1992; 119:945–959. [PubMed: 1385448]

Hing WA, Sherwin AF, Poole CA. The influence of the pericellular microenvironment on the chondrocyte response to osmotic challenge. Osteoarthritis and cartilage / OARS, Osteoarthritis Research Society. 2002; 10:297–307.

Hopf M, Gohring W, Kohfeldt E, Yamada Y, Timpl R. Recombinant domain IV of perlecan binds to nidogens, laminin-nidogen complex, fibronectin, fibulin-2 and heparin. Eur J Biochem. 1999; 259:917–925. [PubMed: 10092882]

Hopf M, Gohring W, Mann K, Timpl R. Mapping of binding sites for nidogens, fibulin-2, fibronectin and heparin to different IG modules of perlecan. J Mol Biol. 2001; 311:529–541. [PubMed: 11493006]

Hunziker EB, Michel M, Studer D. Ultrastructure of adult human articular cartilage matrix after cryotechnical processing. Microsc Res Tech. 1997; 37:271–284. [PubMed: 9185150]

Kavanagh E, Ashhurst DE. Development and aging of the articular cartilage of the rabbit knee joint: Distribution of biglycan, decorin, and matrilin-1. J Histochem Cytochem. 1999; 47:1603–1616. [PubMed: 10567444]

Kielty CM, Whittaker SP, Grant ME, Shuttleworth CA. Type VI collagen microfibrils: evidence for a structural association with hyaluronan. J Cell Biol. 1992; 118:979–990. [PubMed: 1323568]

Kim E, Guilak F, Haider MA. An axisymmetric boundary element model for determination of articular cartilage pericellular matrix properties in situ via inverse analysis of chondron deformation. J Biomech Eng. 2010; 132:031011. [PubMed: 20459199]

Kirn-Safran C, Farach-Carson MC, Carson DD. Multifunctionality of extracellular and cell surface heparan sulfate proteoglycans. Cell Mol Life Sci. 2009; 66:3421–3434. [PubMed: 19629389]

Knight MM, Ross JM, Sherwin AF, Lee DA, Bader DL, Poole CA. Chondrocyte deformation within mechanically and enzymatically extracted chondrons compressed in agarose. Biochim Biophys Acta. 2001; 1526:141–146. [PubMed: 11325535]

Knudson CB. Hyaluronan receptor-directed assembly of chondrocyte pericellular matrix. J Cell Biol. 1993; 120:825–834. [PubMed: 7678838]

Korhonen RK, Herzog W. Depth-dependent analysis of the role of collagen fibrils, fixed charges and fluid in the pericellular matrix of articular cartilage on chondrocyte mechanics. Journal of biomechanics. 2008; 41:480–485. [PubMed: 17936762]

Kvist AJ, Nystrom A, Hultenby K, Sasaki T, Talts JF, Aspberg A. The major basement membrane components localize to the chondrocyte pericellular matrix--a cartilage basement membrane equivalent? Matrix Biol. 2008; 27:22–33. [PubMed: 17825545]

Loparic M, Wirz D, Daniels AU, Raiteri R, Vanlandingham MR, Guex G, Martin I, Aebi U, Stolz M. Micro- and nanomechanical analysis of articular cartilage by indentation-type atomic force microscopy: validation with a gel-microfiber composite. Biophysical journal. 2010; 98:2731–2740. [PubMed: 20513418]

Martin JA, Miller BA, Scherb MB, Lembke LA, Buckwalter JA. Co-localization of insulin-like growth factor binding protein 3 and fibronectin in human articular cartilage. Osteoarthritis and cartilage / OARS, Osteoarthritis Research Society. 2002; 10:556–563.

Melrose J, Hayes AJ, Whitelock JM, Little CB. Perlecan, the “jack of all trades” proteoglycan of cartilaginous weight-bearing connective tissues. Bioessays. 2008; 30:457–469. [PubMed: 18404701]

Melrose J, Roughley P, Knox S, Smith S, Lord M, Whitelock J. The structure, location, and function of perlecan, a prominent pericellular proteoglycan of fetal, postnatal, and mature hyaline cartilages. J Biol Chem. 2006; 281:36905–36914. [PubMed: 16984910]

Melrose J, Smith S, Cake M, Read R, Whitelock J. Perlecan displays variable spatial and temporal immunolocalisation patterns in the articular and growth plate cartilages of the ovine stifle joint. Histochem Cell Biol. 2005; 123:561–571. [PubMed: 16021525]

Michalek AJ, Iatridis JC. A numerical study to determine pericellular matrix modulus and evaluate its effects on the micromechanical environment of chondrocytes. Journal of biomechanics. 2007; 40:1405–1409. [PubMed: 16867304]

Mow VC, Kuei SC, Lai WM, Armstrong CG. Biphasic creep and stress relaxation of articular cartilage in compression: Theory and experiments. J Biomech Eng. 1980; 102:73–84. [PubMed: 7382457]

Poole AR, Pidoux I, Reiner A, Rosenberg L. An immunoelectron microscope study of the organization of proteoglycan monomer, link protein, and collagen in the matrix of articular cartilage. J Cell Biol. 1982; 93:921–937. [PubMed: 7119005]

Poole CA. Articular cartilage chondrons: form, function and failure. Journal of anatomy. 1997; 191 (Pt 1):1–13. [PubMed: 9279653]

Poole CA, Ayad S, Gilbert RT. Chondrons from articular cartilage. V. Immunohistochemical evaluation of type VI collagen organisation in isolated chondrons by light, confocal and electron microscopy. J Cell Sci. 1992; 103 (Pt 4):1101–1110. [PubMed: 1487492]

Poole CA, Ayad S, Schofield JR. Chondrons from articular cartilage: I. Immunolocalization of type VI collagen in the pericellular capsule of isolated canine tibial chondrons. J Cell Sci. 1988; 90 (Pt 4): 635–643. [PubMed: 3075620]

Poole CA, Flint MH, Beaumont BW. Morphological and functional interrelationships of articular cartilage matrices. Journal of anatomy. 1984; 138 (Pt 1):113–138. [PubMed: 6706831]

Poole CA, Flint MH, Beaumont BW. Chondrons in cartilage: ultrastructural analysis of the pericellular microenvironment in adult human articular cartilages. J Orthop Res. 1987; 5:509–522. [PubMed: 3681525]

Poole CA, Gilbert RT, Herbage D, Hartmann DJ. Immunolocalization of type IX collagen in normal and spontaneously osteoarthritic canine tibial cartilage and isolated chondrons. Osteoarthritis and cartilage / OARS, Osteoarthritis Research Society. 1997; 5:191–204.

Radmacher M, Tillamnn RW, Fritz M, Gaub HE. From molecules to cells: imaging soft samples with the atomic force microscope. Science. 1992; 257:1900–1905. [PubMed: 1411505]

Smith SM, West LA, Govindraj P, Zhang X, Ornitz DM, Hassell JR. Heparan and chondroitin sulfate on growth plate perlecan mediate binding and delivery of FGF-2 to FGF receptors. Matrix Biol. 2007; 26:175–184. [PubMed: 17169545]

Soder S, Hambach L, Lissner R, Kirchner T, Aigner T. Ultrastructural localization of type VI collagen in normal adult and osteoarthritic human articular cartilage. Osteoarthritis and cartilage / OARS, Osteoarthritis Research Society. 2002; 10:464–470.

SundarRaj N, Fite D, Ledbetter S, Chakravarti S, Hassell JR. Perlecan is a component of cartilage matrix and promotes chondrocyte attachment. J Cell Sci. 1995; 108 (Pt 7):2663–2672. [PubMed: 7593307]

Tillet E, Wiedemann H, Golbik R, Pan TC, Zhang RZ, Mann K, Chu ML, Timpl R. Recombinant expression and structural and binding properties of alpha 1(VI) and alpha 2(VI) chains of human collagen type VI. Eur J Biochem. 1994; 221:177–185. [PubMed: 8168508]

Villanueva I, Weigel CA, Bryant SJ. Cell-matrix interactions and dynamic mechanical loading influence chondrocyte gene expression and bioactivity in PEG-RGD hydrogels. Acta biomaterialia. 2009; 5:2832–2846. [PubMed: 19508905]

Vincent T, Hermansson M, Bolton M, Wait R, Saklatvala J. Basic FGF mediates an immediate response of articular cartilage to mechanical injury. Proceedings of the National Academy of Sciences of the United States of America. 2002; 99:8259–8264. [PubMed: 12034879]

Vincent TL, Hermansson MA, Hansen UN, Amis AA, Saklatvala J. Basic fibroblast growth factor mediates transduction of mechanical signals when articular cartilage is loaded. Arthritis Rheum. 2004; 50:526–533. [PubMed: 14872495]

Vincent TL, McLean CJ, Full LE, Peston D, Saklatvala J. FGF-2 is bound to perlecan in the pericellular matrix of articular cartilage, where it acts as a chondrocyte mechanotransducer. Osteoarthritis and cartilage / OARS, Osteoarthritis Research Society. 2007; 15:752–763.

Whitelock JM, Melrose J, Iozzo RV. Diverse cell signaling events modulated by perlecan. Biochemistry. 2008; 47:11174–11183. [PubMed: 18826258]

Whitelock JM, Murdoch AD, Iozzo RV, Underwood PA. The degradation of human endothelial cell-derived perlecan and release of bound basic fibroblast growth factor by stromelysin, collagenase, plasmin, and heparanases. J Biol Chem. 1996; 271:10079–10086. [PubMed: 8626565]

Wiberg C, Heinegard D, Wenglen C, Timpl R, Morgelin M. Biglycan organizes collagen VI into hexagonal-like networks resembling tissue structures. J Biol Chem. 2002; 277:49120–49126. [PubMed: 12354766]

Wilusz RE, DeFrate LE, Guilak F. Immunofluorescence-guided atomic force microscopy to measure the micromechanical properties of the pericellular matrix of porcine articular cartilage. J R Soc Interface. in press.

Highlights

- Type VI collagen and perlecan in the cartilage PCM were immunolabeled.
- Atomic force microscopy used to measure microscale elastic properties.
- Interior PCM regions rich in type VI collagen and perlecan exhibit lower moduli.
- Enzymatic removal of heparan sulfate increases moduli of interior PCM regions.
- Perlecan may be defining factor in the boundary of the cartilage PCM.

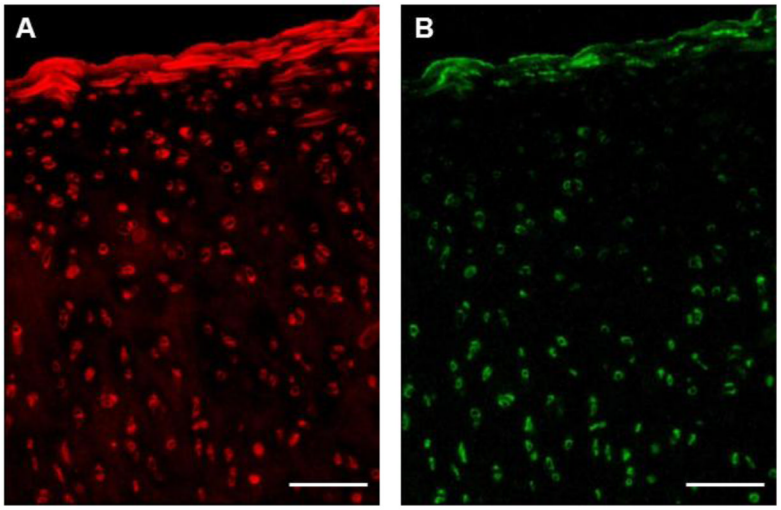

Figure 1.
Immunofluorescence labeling of unfixed sections of porcine articular cartilage. (A) Staining for type VI collagen was uniform throughout the cartilage thickness in pericellular regions and faintly dispersed in the ECM in deeper regions. (B) Perlecan labeling was localized to pericellular regions and more pronounced in the middle and deep zones. Scale bar = 100 μm.

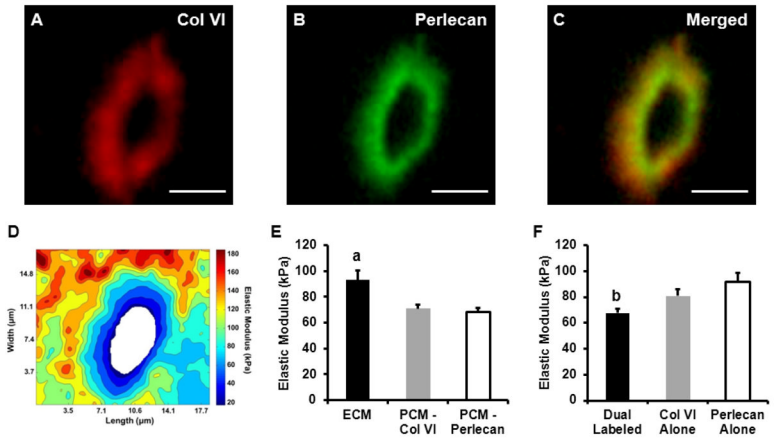

Figure 2.

AFM stiffness mapping of PCM regions dual-labeled for type VI collagen and perlecan. A representative PCM scan region in the middle/deep zone is shown. Dual IF-labeling for (A) type VI collagen and (B) perlecan demonstrated the (C) co-localization of these molecules in the pericellular space. Scale bar = 5 μm. (D) Contour map of calculated elastic moduli for the PCM scan region shown. (E) Elastic moduli of cartilage ECM and PCM as defined by the presence of type VI collagen or perlecan. There was no difference between biochemical definitions of the PCM ($p = 0.70$). ECM elastic moduli were significantly greater than PCM moduli (a: $p < 0.005$ as compared to either PCM definition). (F) Within the PCM regions, dual-labeled for type VI collagen and perlecan exhibited lower elastic moduli than regions positive for type VI collagen or perlecan alone (b: $p < 0.05$ as compared to type VI collagen and perlecan alone regions). Data presented as Mean + SEM ($n \geq 9$).

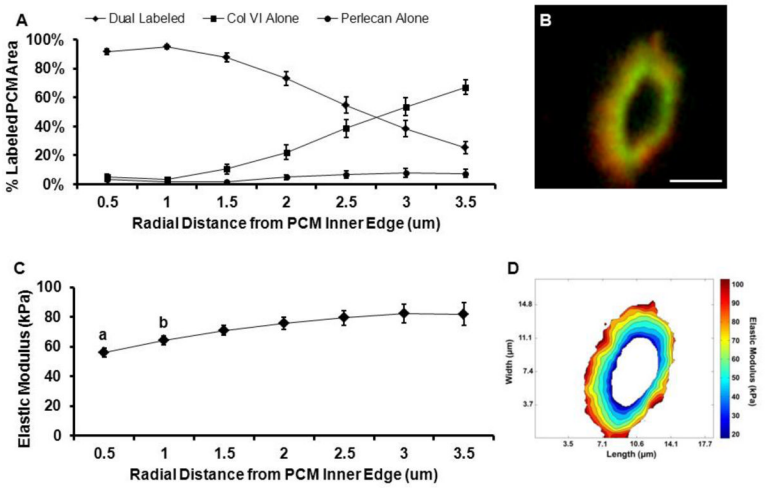

Figure 3.

Spatial distribution of PCM biochemical composition and micromechanical properties from the PCM inner edge. Evaluation was performed at radial increments of 0.5 μm. (A) Outward progression of PCM biochemical composition. Within each radial increment, data represent the relative composition based on the percent of total IF labeled PCM area occupied by each antibody/antibody combination. (B) Representative IF labeling demonstrating co-localization of type VI collagen (red) and perlecan (green) within the PCM. Scale bar = 5 μm. (C) Outward stiffness progression of PCM elastic moduli. Elastic moduli within 1.0 μm from the PCM inner edge were less than moduli in peripheral regions (a: $p < 0.05$ as compared to distances greater than 1.5 μm; b: $p < 0.05$ as compared to distances greater than 2.5 μm). (D) Contour map of calculated elastic moduli within the PCM scan region shown in panel B. Data presented as Mean ± SEM (n = 23).

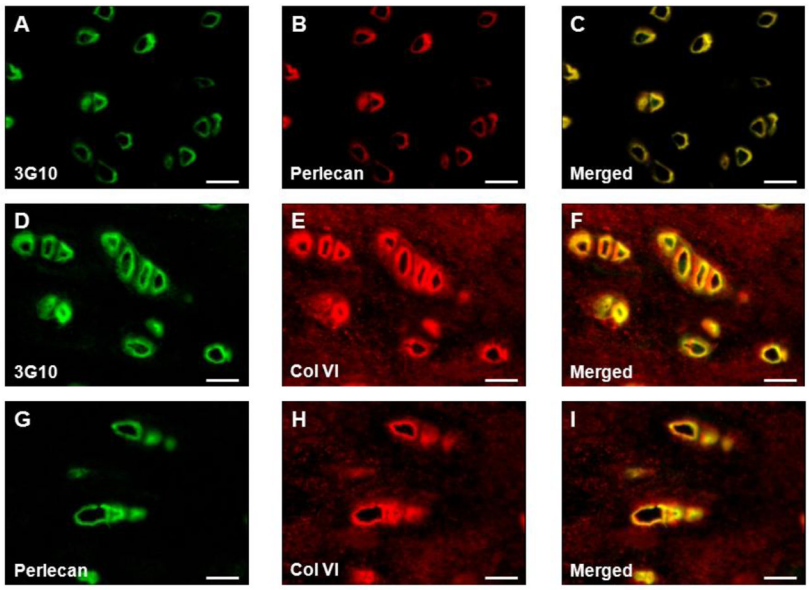

Figure 4.

Immunofluorescence labeling of unfixed porcine cartilage sections following heparinase III. Dual IF labeling of (A) HS epitope 3G10 and (B) perlecan exhibited a nearly one-to-one overlay (C). (D) 3G10 and (E) type VI collagen co-localized in the pericellular space around cell-voids (F). Heparinase III digestion had no effect on labeling of (G) perlecan or (H) type VI collagen and did not disrupt their co-localization in the PCM (I). Scale bar = 20 μm.

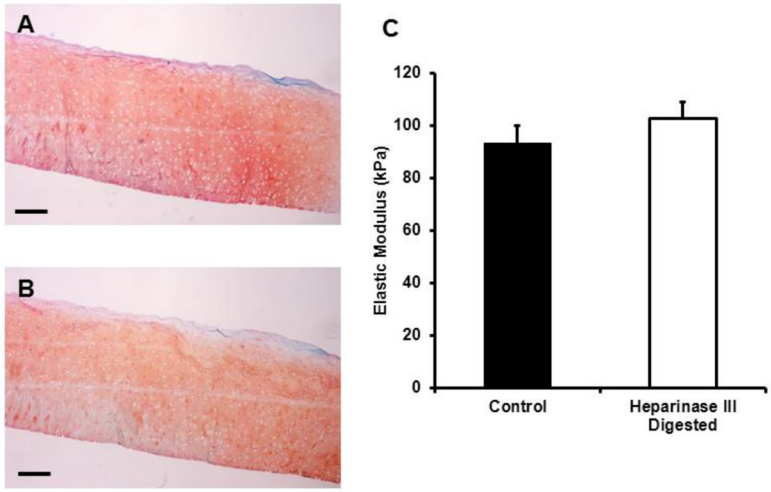

Figure 5.

Effect of heparinase III digestion on ECM composition and micromechanical properties. (A) Histological staining with safranin-O (red, proteoglycans) and fast green (blue, collagens) demonstrated that digestion with heparinase III had a minimal effect on global proteoglycan content as compared to (B) undigested control. Scale bar = 250 μm. (C) ECM elastic moduli were unaffected by heparinase III digestion ($p = 0.39$). Data presented as Mean + SEM ($n = 25$).

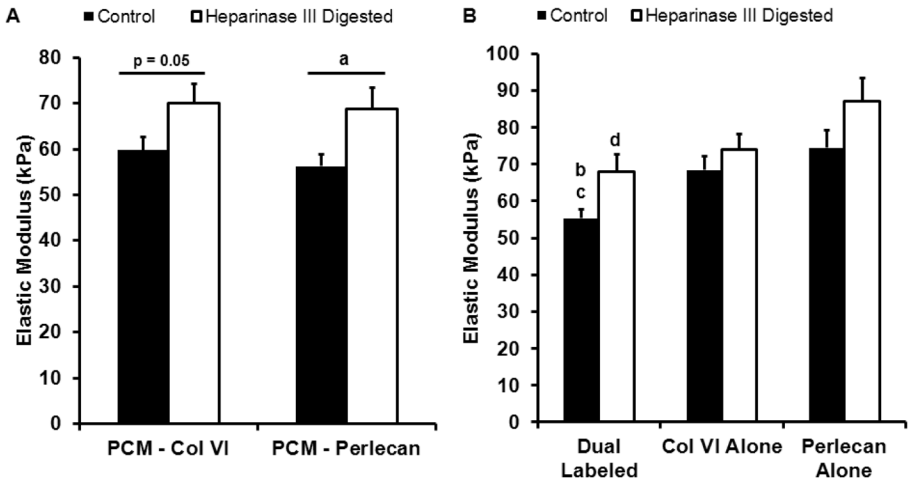

Figure 6.

Effect of heparinase III digestion on PCM micromechanical properties. (A) PCM moduli as defined by perlecan significantly increased with heparinase III digestion (a: $p < 0.05$ as compared to control). PCM moduli as defined by type VI collagen showed a trend toward higher moduli with digestion ($p = 0.05$ as compared to control). (B) Within the PCM, elastic moduli of dual-labeled regions significantly increased with heparinase III digestion (b: $p < 0.05$ as compared to digested). In undigested controls, dual-labeled regions exhibited elastic moduli that were significantly less than regions positive for type VI collagen or perlecan alone (c: $p < 0.05$ as compared to undigested type VI collagen and perlecan alone regions). In digested samples, elastic moduli in dual-labeled regions were significantly less than those in regions positive for perlecan alone (d: $p < 0.05$ as compared to undigested perlecan alone). Data presented as Mean + SEM ($n \geq 13$).

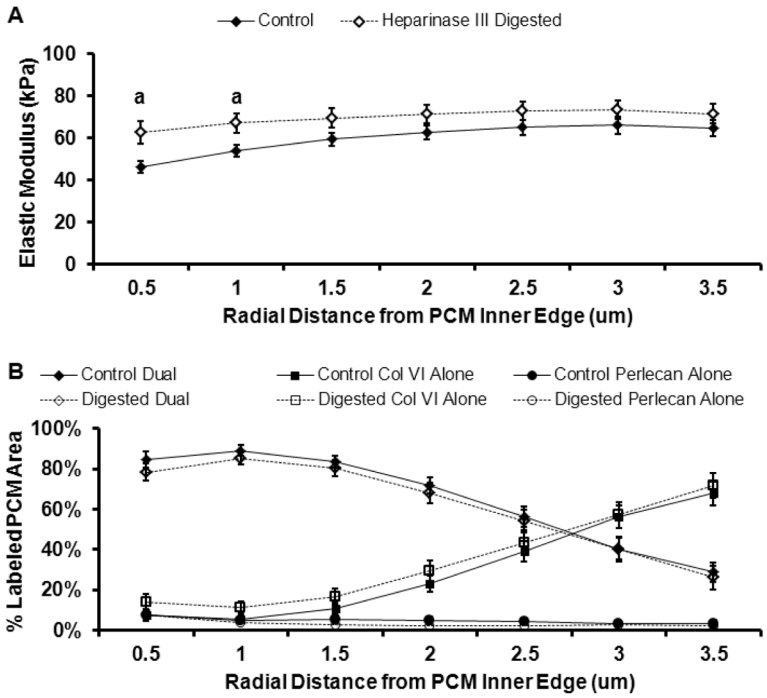

Figure 7.

Effect of heparinase III digestion on the spatial distribution of PCM elastic properties. Evaluation was performed at radial increments of 0.5 μm from the PCM inner edge. (A) Outward stiffness progression of PCM elastic moduli from the PCM inner edge for control (black) and digested (white) samples. Regions within 1.0 μm from the PCM inner edge exhibited higher elastic moduli with heparinase III digestion as compared to undigested controls (a: $p < 0.05$ for digested as compared undigested controls). (B) Outward progression of biochemical composition from the PCM inner edge for control (black) and digested (white) samples. Within each radial increment, data represent the relative composition based on the percent of total IF labeled PCM area occupied by each antibody/antibody combination. Data presented as Mean ± SEM (n = 25).